Dynamic Performance of Duolayers at the Air/Water Interface – Part B: Mechanistic Insights from All-atom Simulations.

ARTICLE *in* THE JOURNAL OF PHYSICAL CHEMISTRY B · AUGUST 2014

Impact Factor: 3.3 · DOI: 10.1021/jp506098d · Source: PubMed

8 AUTHORS, INCLUDING:

Andrew J. Christofferson
RMIT University
17 PUBLICATIONS **52** CITATIONS
SEE PROFILE

George Yiapanis
IBM
23 PUBLICATIONS **124** CITATIONS
SEE PROFILE

Emma L Prime
University of Melbourne
17 PUBLICATIONS **159** CITATIONS
SEE PROFILE

Irene Yarovsky
RMIT University
154 PUBLICATIONS **2,245** CITATIONS
SEE PROFILE

THE JOURNAL OF PHYSICAL CHEMISTRY B

Article

pubs.acs.org/JPCB

Dynamic Performance of Duolayers at the Air/Water Interface. 2. Mechanistic Insights from All-Atom Simulations

Andrew J. Christofferson,[†] George Yiapanis,[†,§] Andy H. M. Leung,[‡] Emma L. Prime,[‡] Diana N. H. Tran,[‡] Greg G. Qiao,[‡] David H. Solomon,[‡] and Irene Yarovsky*[,†]

[†]School of Aerospace, Mechanical and Manufacturing Engineering, RMIT University, GPO Box 2476, Melbourne, VIC 3001, Australia

[‡]Department of Chemical & Biomolecular Engineering, The University of Melbourne, Parkville, VIC 3010, Australia

ABSTRACT: The novel duolayer system, comprising a monolayer of ethylene glycol monooctadecyl ether (C18E1) and the water-soluble polymer poly(vinylpyrrolidone) (PVP), has been shown to resist forces such as wind stress to a greater degree than the C18E1 monolayer alone. This paper reports all-atom molecular dynamics simulations comparing the monolayer (C18E1 alone) and duolayer systems under an applied force parallel to the air/water interface. The simulations show that, due to the presence of PVP at the interface, the duolayer film exhibits an increase in chain tilt, ordering, and density, as well as a lower lateral velocity compared to the monolayer. These results provide a molecular rationale for the improved performance of the duolayer system under wind conditions, as well as an atomic-level explanation for the observed efficacy of the duolayer system as an evaporation suppressant, which may serve as a useful guide for future development for thin films where resistance to external perturbation is desirable.

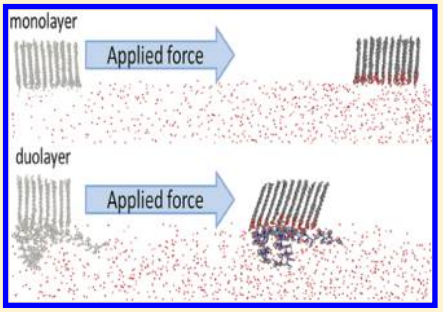

INTRODUCTION

Monolayers have a wide variety of applications in a diverse range of fields, from biosensing[1] and drug delivery[2] in medicine to property-altering coatings for surfaces[3] and electromechanical devices.[4] Composed of chain molecules with a headgroup, tail, and possibly a functional group at the end of the tail, monolayers are versatile due to the sheer number of possible atomic configurations of the individual chains. Of particular interest is the performance of monolayers under various conditions, such as gas/liquid flow,[5] friction/loading,[6] diffusion,[7] protein binding,[8] and self-assembled monolayer formation.[9] An understanding of monolayer properties under various stressors is critical to designing useful, stable, and efficient monolayers.

Nonequilibrium molecular dynamics (NEMD) allows for an atomic-level understanding of systems under stress. For example, Ramin et al. examined alkanethiol self-assembled monolayers on gold surfaces under various loading and shearing conditions and found an odd−even effect relating the number of carbons in the aliphatic chain to the friction coefficient. They also described a clear stick−slip pattern in the shear stress, film thickness, and tilt of the monolayer.[10] Song et al. found that the Stokes−Einstein equation relating molecular diffusion to viscosity is valid for a single nanoparticle at a water/oil interface, and that lateral diffusion of nanoparticles at the interface is independent of their position at the interface.[11]

In this study, we use nonequilibrium molecular dynamics to simulate the effects of wind on a monolayer spread over a water surface to prevent evaporation from large open-air water storages.[12] The evaporation suppression properties of monolayers on water have been studied since 1925,[13] but attempts to create an efficient and commercially viable monolayer compound that mitigates water evaporation for sufficiently long periods of time have been met with difficulties. Many monolayer candidates developed in the lab failed to perform adequately in field trials, often due to wind and wave action.[14] Attempts to overcome this have included the use of comb polymers and comb/monolayer blends,[15] manipulating the anchoring ability of the monolayer headgroup,[16] and monolayer/monolayer blends.[17] Recently, we discovered that water-soluble surface-active polymers can noncovalently interact with the monolayer to form a so-called "duolayer".[18,19] The duolayer system of an ethylene glycol monooctadecyl ether (C18E1, IUPAC name 2-(octadecyloxy)ethanol) monolayer combined with the polymer poly(vinylpyrrolidone) (PVP) exhibits similar evaporation reduction performance and packing density to a C18E1 monolayer under static conditions. Interestingly, canal viscometry experiments have shown that the duolayer has a greater surface viscosity than the monolayer,[19] which suggested it may be more stable under wind. This two-part (1 and 2) publication series aims to examine the dynamic performance of the duolayer systems experimentally (part 1)[20] and elucidate the molecular mechanisms of its behavior theoretically using all-atom NEMD simulations, presented herein (part 2).

Received: June 19, 2014
Revised: July 28, 2014
Published: August 25, 2014

The experimental data on the dynamic performance of the three-monolayer and three-duolayer systems presented in part 1 of this two-part series[20] show that, under wind conditions, not only does the duolayer outperform the monolayer as an evaporation suppressant, but it also outperforms itself under stationary conditions. Here, we use classical molecular dynamics techniques to compare the interfacial properties of the monolayer and duolayer systems under equilibrium and applied force conditions. By applying a force parallel to the water surface, we aim to simulate the effects of wind on the monolayer and duolayer systems and compare them across the range of properties associated with evaporation suppression performance of monolayers and duolayers for the equilibrium systems studied previously.[16,21]

EXPERIMENTAL SECTION

Computational Models of Thin Films. The initial models of the monolayer and duolayer systems comprised a one molecule thick layer of 80 ethylene glycol monooctadecyl ether (C18E1) chains on top of a water layer of at least 45 Å in thickness. The water phase was equilibrated at a density of 1 g/cm^3 from initial random packing in a 3D unit cell.[22] We applied three-dimensional periodic boundary conditions to the monolayer/duolayer systems, with a vacuum space of at least 40 Å in the z-direction to mimic a two-dimensional interface. Periodic unit cell dimensions of 40.5 × 40.5 × 140 Å^3 yielded a monolayer packing density of 20.5 Å^2 per molecule, which is the equilibrium packing density of C18E1 at surface pressures of ~25−50 mN/m.[19] Details of the monolayer model packing procedure can be found elsewhere.[23] The duolayer system was created by randomly positioning four PVP oligomers of 20 monomer units each (average molecular weight of 2224.9 g/mol) at an average initial distance of no less than 15 Å from the film in the water layer, similar to the previously studied equilibrium systems.[21] The initial polymer configurations in aqueous solution were generated by the Theodorou-Suter method.[22]

Simulation Details. Four systems were studied in this work (Figure 1): (1) monolayer under equilibrium conditions (Eq-Monolayer), (2) duolayer under equilibrium conditions (Eq-Duolayer), (3) monolayer under an applied force (Af-Monolayer), and (4) duolayer under an applied force (Af-Duolayer).

For the dynamic performance experiments in part 1 (DOI 10.1021/jp5060974), three-monolayer or three-duolayer systems were used due to the increased surface area caused by wave creation. However, the main water surface is covered only by one monolayer or one duolayer, as shown by Brewster angle microscopy.[20] Therefore, in the molecular simulations, only one monolayer or one duolayer is used, as only a small time frame (50 ns) and surface area (1640 Å^2) are examined, without any change in surface area during simulation. The starting monolayer chain configurations were taken from previously modeled liquid-condensed states of the aliphatic chains, characterized by a tightly packed chain arrangement, typical of equilibrium surface pressure.[21] The simulations were performed using the LAMMPS MD code[24] with the polymer consistent force field (PCFF),[25,26] an *ab initio* force field developed to cover a broad range of organic molecules and polymers. PCFF has been shown to reproduce density, solubility parameters, free energy of binding, and glass transition temperatures for a wide range of polymers,[27] including vinyl-based polymers relevant to this study.[28−30]

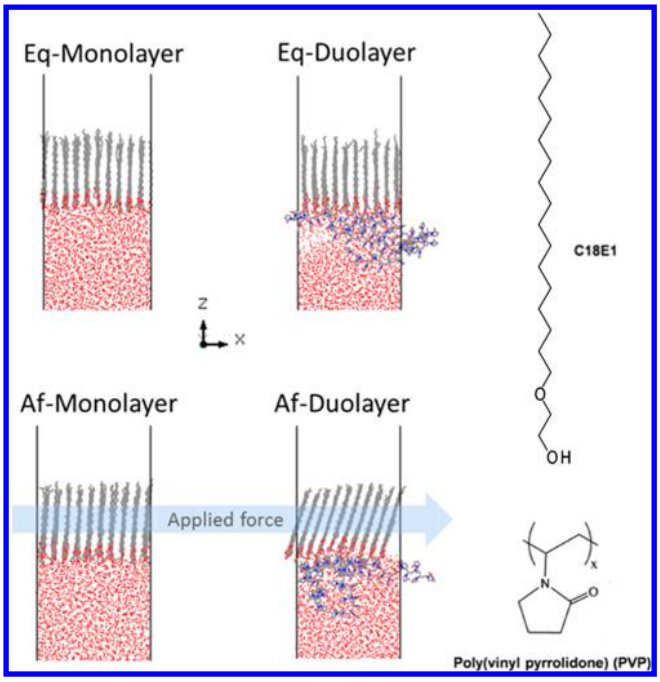

Figure 1. Schematic diagram of the monolayer and duolayer systems at equilibrium (Eq) and with an applied force (Af). Also shown are the chemical structures of ethylene glycol monooctadecyl ether (C18E1) and poly(vinylpyrrolidone) (PVP).

PCFF has been previously used to model polymer−water interactions[31] and monolayer properties[32−35] including monolayer surfactants on water.[36] We have previously used PCFF to model the duolayer systems at equilibrium.[21] In this work, the nonbond interactions were evaluated with a cutoff distance of 15.50 Å for the real space portion, with the particle−particle particle−mesh solver (PPPM) method[37] for long-range electrostatics and a tail correction for long-range van der Waals interactions. The Nosé−Hoover thermostat[38,39] was used to maintain a constant temperature of 298 K.

All simulations were performed with a 1.0 fs time step. We employed the NVT ensemble to sustain the C18E1 packing density, as this best mimics the experimental conditions, where the equilibrium area per molecule was maintained throughout the experiment.[20] Trajectories were generated by saving atomic coordinates in 10 ps time intervals. The Eq-Monolayer and Eq-Duolayer systems were simulated for a total time of 50 ns, and considered equilibrated when the standard deviation of the total energy was within 1% of the average, the monolayer tilt reached a steady value, and for the duolayer systems when the PVP center of mass reached a steady z-position at the interface.[21] The short time scale dynamic properties (hydrogen bond lifetimes and mean squared displacement for subdiffusive translational motion evaluation) were calculated on equilibrated trajectories for 100 ps with the data saved every 0.1 ps.

In order to simulate the pressure exerted on the monolayer by wind blowing at approximately 25 km/h, a force of 5 × 10^{-6} kcal/mol·Å was applied to the carbon atoms of the C18E1 film in the positive x-direction, with a viscous damping force of 0.5 kcal·fs/mol·Å^2 applied to the same atoms to provide a constant velocity. The Af-Monolayer and Af-Duolayer systems were fully equilibrated prior to applying the force and then run for a total of 12 ns under the force. Simulations were also performed with the force applied in the positive y-direction, with results within

dx.doi.org/10.1021/jp506098d | J. Phys. Chem. B 2014, 118, 10927−10933

statistical variations (i.e., standard deviation) for each property examined.

To examine the hydrogen bonding network at the film/water interface, we employed a geometric criterion to define a hydrogen bond (H-bond) between donor−acceptor pairs with a H-bond said to exist if the distance between the hydrogen and the acceptor is less than 2.5 Å and the donor−hydrogen−acceptor angle is greater than 120°. Further details of the calculation of H-bond statistics and lifetimes may be found elsewhere.[21,40]

To ensure that our results were not an artifact of the ensemble, we performed additional NPT (constant pressure and temperature) simulations for each model system. Pressure tensors were applied in the x and y directions to generate a semi-isotropic ensemble with a packing density similar to that of the NVT simulations (~20.5 Å^2 per C18E1 molecule). All other conditions were identical to the NVT systems.

RESULTS AND DISCUSSION

When a force is applied to the C18E1 film, in both the monolayer and duolayer systems, the C18E1 chains move in the direction of the force. There is a significant (27%) difference in the average film velocities, with a value of 1.77 m/s for the Af-Monolayer system and 1.29 m/s for the Af-Duolayer system, indicating that there is an increase in film viscosity with incorporation of PVP, in qualitative agreement with experiment.[19,20] Experimentally, it has been estimated that the velocity of a monolayer under wind is approximately 2% of the wind velocity (~0.1 m/s).[41] The velocities simulated in this study were higher than the estimated values, which ensured that any observed differences in the systems are statistically meaningful within the nanosecond time scale examined and provide qualitative comparison between the systems examined. We also note that applying greater forces in the simulations was not feasible, as the signal-to-noise ratio for the properties of interest was reduced beyond the point of extracting meaningful data (results not shown).

Interdigitation. We expect the surface viscosity of the monolayer film to be strongly influenced by interdigitation, loosely defined as any type of interdiffusion or interpenetration occurring at the interface that increases the number of contacts between the molecular groups across the film/subphase boundary. In the case of the duolayer system, we observe interpenetration of PVP and C18E1 at the film/water interface (Figure 2). This in turn increases the atomic density across this region (Figure 3).

Moreover, the PVP is dragged together with the aliphatic chains along the interface, as reflected in the mean squared displacement (MSD) curves of Figure 4. The sliding plane is therefore no longer linear, giving rise to a high frictional force as the PVP and chain headgroups "plough" though the water phase during sliding. It has been previously shown[42−45] that chains from one surface do not have to penetrate by more than a few angstroms into the other surface for frictional forces to be significant, and we therefore expect the surface viscosity of the film to be greatly increased due to even a small degree of interpenetration of the C18E1 chains and PVP polymer. This effect is dependent on the amount of PVP present at the interface, and has been shown experimentally to decrease over time as PVP migrates away from the water surface.[20] In contrast, in the absence of PVP, the viscosity is lower, since the density at the film−water interface is lower (Figure 3). It can be suggested that this is the result of smaller frictional forces between the monolayer chains and water subphase relative to the polymer supported monolayer systems.

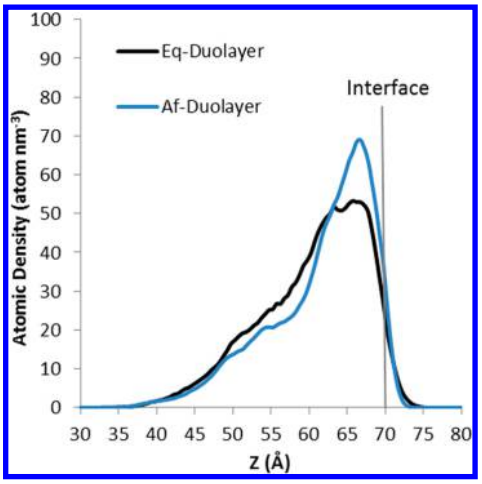

Figure 2. Atomic concentration profiles of PVP along the direction perpendicular to the interface plane, indicating an increase in interdigitation between the PVP and C18E1 film under an applied force. The interface plane between the C18E1 film and subphase (water and PVP) is normalized to 70 Å for both systems.

Film Arrangement. All films display a hexagonal arrangement of aliphatic chains, irrespective of the presence of PVP or external perturbation (Figure 5).

However, the molecular tilt of the chains is seen to increase under an applied stress, with the duolayer system displaying the most prominent increase in molecular tilt ($\Delta\theta$ = 7.8°) in contrast to its monolayer counterpart ($\Delta\theta$ = 3.0°) (Table 1).

This overall increase in molecular tilt is accompanied by a reduction in tilt angle standard deviation between individual chains, indicating less fluctuation within the film under an external force. This is particularly notable in the case of the duolayer system. Closer examination of the molecular arrangement of the chains within the film suggests that only under an external stress and in the presence of PVP the chains can adopt a next nearest neighbor tilt (NNN, Figure 5), which explains the higher molecular tilt of the duolayer system (Af-Duolayer). This is in accordance with previous X-ray diffraction studies of tilted fatty acid monolayers which have shown[46,47] that, at high surface pressures when the molecule tilts toward its NNN rather than to its nearest neighbor (NN), the tilt angle increases. In the absence of PVP, the aliphatic chains exhibit a NN tilt irrespective of external perturbation.

Film Stability. The stability of the aliphatic film will be dependent on the frictional forces at the sliding interface (discussed above) as well as the interactions within the film itself, which is the focus of this discussion. We have shown that, under an external force, the aliphatic molecules of the duolayer systems pack with a slight tilt with respect to the surface rather than stand upright. This reduces the actual thickness of the film in the z-direction and, in the absence of an increase in the area per molecule, leads to a higher density of the film, as shown in Figure 3. While some increase in chain density is also observed in the monolayer system, the magnitude is far smaller compared to its duolayer counterpart. The rise in density can be expected to further stabilize the film under an external force. We note that the same trend was observed in simulations employing the NPT ensemble, with an increase in film density under external force that is augmented in the presence of PVP. All other

dx.doi.org/10.1021/jp506098d | J. Phys. Chem. B 2014, 118, 10927−10933

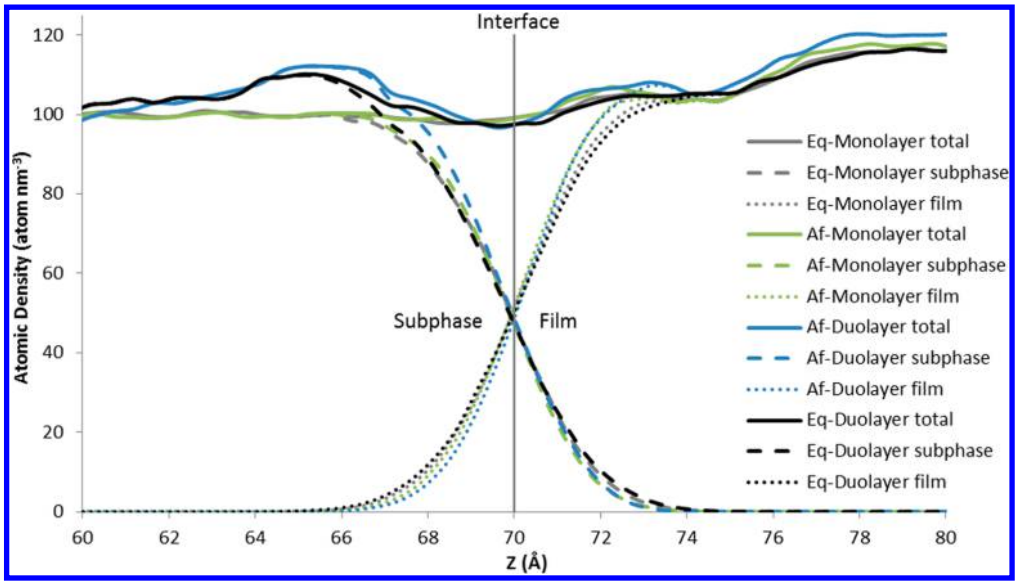

Figure 3. Atomic concentration profiles of the monolayer and duolayer systems along the direction perpendicular to the interface plane at equilibrium and under an applied force. The presence of PVP increases the atomic density of the subphase for the Eq- and Af-Duolayer systems (black and blue lines). An applied force increases the atomic density in the subphase and film for the Af-Duolayer system (blue lines) and in the film only for the Af-Monolayer system (green lines). The interface plane between the C18E1 film and subphase is normalized to 70 Å for all systems.

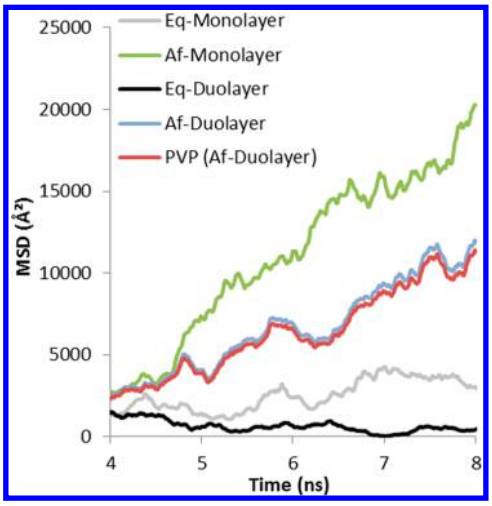

Figure 4. Mean squared displacement (MSD) of the C18E1 carbon atoms for the monolayer and duolayer systems at equilibrium and with an applied force and PVP carbon atoms for the duolayer system with an applied force.

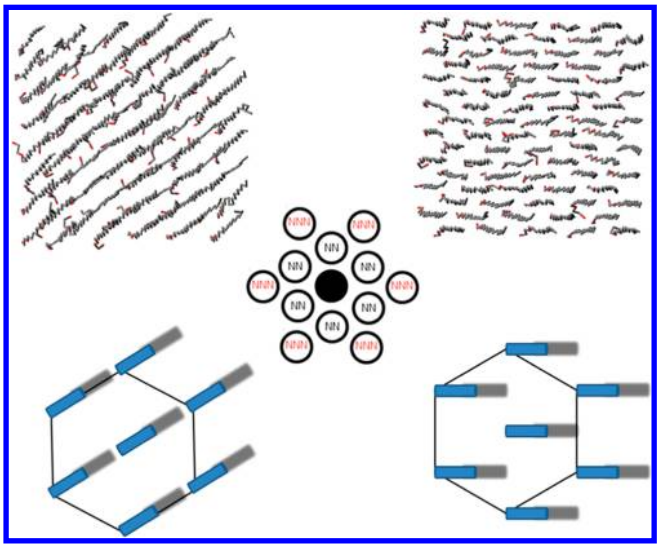

Figure 5. Simulation snapshot (top) and schematic (bottom) of nearest neighbor (NN, left) and next nearest neighbor (NNN, right) C18E1 tilt. Under an applied force, the C18E1 film of the duolayer system transitions from a NN tilt to a NNN tilt, accompanied by an increase in tilt angle. The monolayer exhibits a NN tilt in both equilibrium and applied force simulations. In the simulation shapshots, carbons are shown in gray and oxygens in red.

property trends for the NPT simulations were in agreement with those of the NVT ensemble (results not shown).

Energies for the film chain−chain interactions, calculated as a difference between the total potential energy of the C18E1 film and the sum of the potential energies for each individual chain, are shown in Table 1. There is little difference in the per-chain energy between the monolayer and duolayer systems at equilibrium. However, in the systems with the force applied, the energy is enhanced by 1.79 ± 0.02 kcal/mol per chain for the duolayer system and by 0.55 ± 0.02 kcal/mol per chain for the monolayer system. This indicates a strengthening of the chain−chain interactions of the film under stress, and the effect is considerably greater in the duolayer system where the density of the chains increases to a greater extent.

To further understand the stabilization within the film, we examine the chain headgroup geometry under equilibrium and

Table 1. Average Molecular Tilt (θ) and Relative Energies of the Chain−Chain Interactions of the C18E1 Chains in the Monolayer and Duolayer Systems[a]

	θ (deg)	standard deviation (deg)	energy of chain−chain interaction (kcal/mol)
Eq-Monolayer	9.40	2.06	
Af-Monolayer	12.38	1.39	−0.55 ± 0.28
Eq-Duolayer	9.13	2.19	−0.26 ± 0.30
Af-Duolayer	17.10	1.05	−2.05 ± 0.28

[a]Energies are given per chain, and relative to the Eq-Monolayer system.

dx.doi.org/10.1021/jp506098d | J. Phys. Chem. B 2014, 118, 10927−10933

applied force conditions. Figure 6 presents the oxygen−oxygen radial distribution function (RDF) for the C18E1 head groups.

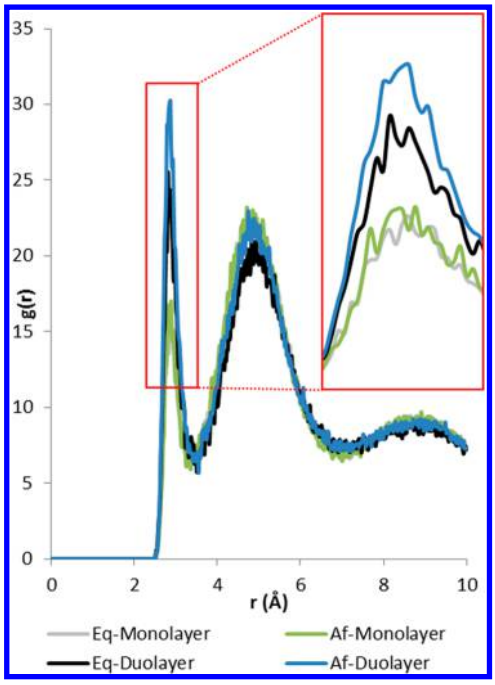

Figure 6. Radial distribution functions of the C18E1 headgroup oxygen atoms.

It shows an increased correlation between head groups when PVP is in close proximity to the externally perturbed film. This indicates that, under applied force conditions, the head groups of the C18E1 chains are far more ordered when PVP is present. This effect is also confirmed by the analysis of the chain−chain H-bond lifetimes. For the monolayer system, there is only a small increase in the interchain H-bond lifetime, from 0.97 to 1.1 ps, while for the duolayer system the lifetime increases from 1.53 to 3.8 ps when a force is applied. Previous studies have shown that the preferred tilt angle and tilt direction depend on the headgroup lattice spacing,[48] and as the symmetry of the headgroup lattice increases, the C18E1 film viscosity increases.[49] Thus, the increase in ordering of the C18E1 head groups in the duolayer system under an applied force may account for the observed changes in tilt angle and orientation, as well as the increase in film viscosity, observed experimentally.[20]

Interestingly, while the chain head groups are more ordered in the duolayer system, carbon−carbon RDFs for the C18E1 (Figure 7) reveal that there is no significant difference in the ordering of the aliphatic tails of the chains between the monolayer and duolayer systems at equilibrium.

However, under an applied force, there is an increase in chain ordering in both systems but more so in the Af-Duolayer system. The C18E1 carbon−carbon RDFs confirm the trends observed for the chain−chain interaction energies (Table 1), suggesting that the aliphatic chains attain more order and stability only when an external force is applied. This is in contrast with the headgroup behavior, where the presence of the PVP was shown to stabilize the head groups regardless of an applied force.

Interfacial Water Dynamics. The mobility of interfacial water can be more thoroughly examined through the

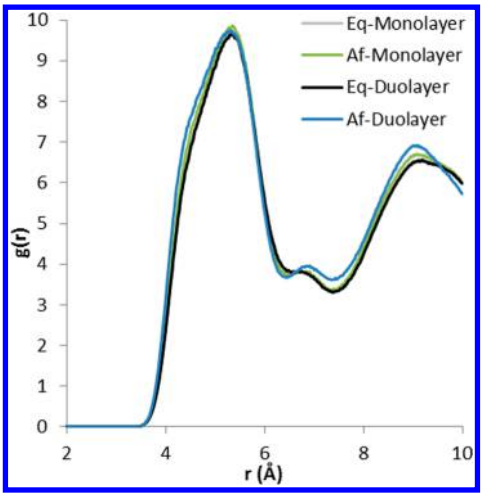

Figure 7. Carbon−carbon radial distribution functions of the C18E1 aliphatic carbons for the monolayer and duolayer systems at equilibrium and under an applied force. Both the monolayer and duolayer aliphatic chains are more ordered under an applied force, as shown by an increase in $g(r)$.

intermittent H-bond correlation function of chain-water groups at the film−water interface (Figure 8).

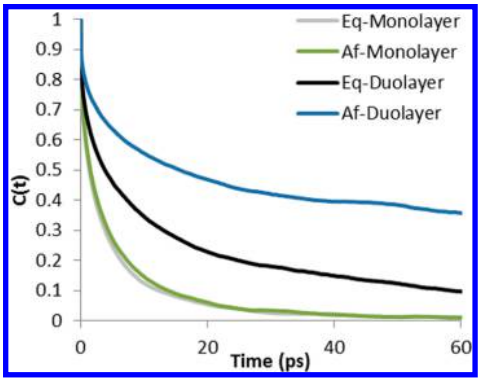

Figure 8. Intermittent H-bond correlation function for chain-water groups at the film−water interface.

The intermittent H-bond correlation function gives the probability that a particular hydrogen bond will be intact at time t, given it was present at time zero. It accounts for the breaking of and reforming of H-bonds, and in the context of this study, it provides information about the dynamics of hydrogen bonds between monolayer chains and water which is strongly coupled with the difference in diffusive behavior of the two molecular groups. When a hydrogen bond between two molecules is broken, the molecules may remain in close contact if the hydrogen bond is reformed; otherwise, they may diffuse away from each other. Intermittent H-bond lifetimes are defined here as the time taken for the correlation function $C(t)$ to reach e^{-1} (~0.37). Figure 8 shows that, in the absence of PVP (monolayer system), the external stress has little effect on the chain-water dynamics, resulting in only a marginal increase in intermittent H-bond lifetime from 2.75 to 3.05 ps. Therefore, water molecules appear to remain in close contact with the sliding interface for a short period before they diffuse away. However, when the same external force is applied to the duolayer system, the intermittent H-bond lifetime is increased almost an order of magnitude from 8.7 to 54.5 ps, indicating a

dx.doi.org/10.1021/jp506098d | J. Phys. Chem. B 2014, 118, 10927−10933

significant slowing down of the molecular relaxation time of water-chain H-bonds. This is likely due to the greater ordering of the C18E1 head groups in the duolayer system. Compared to the monolayer, the duolayer system demonstrates a much less frequent exchange between interfacial and bulk water, indicative of higher friction and reduced mobility along the slip plane. This is in good agreement with the canal viscosity experiments, which show that the duolayer moves across the surface of the water and through the canal at a slower rate than the monolayer.[19,20]

Mechanism of Improved Water Evaporation Suppression. There are two possible explanations for the experimentally observed improvement in water evaporation suppression by the duolayer system under wind compared to both the monolayer under wind and the duolayer itself in the absence of wind: (1) the PVP simply provides a greater mechanical retention (anchoring) of the C18E1 film, and (2) changes in the molecular properties of the duolayer film under wind stress provide a more effective barrier to water evaporation. If only (1) were true, we would expect the monolayer and duolayer to perform similarly at the beginning of the experiment when the C18E1 films in both systems have good coverage of the water, but over time, the duolayer should start to outperform the monolayer as more C18E1 is lost from the monolayer system. Instead, we observe that the duolayer presents a stronger barrier to evaporation even at the beginning of the experiment when the C18E1 layers in both systems have similar concentrations and surface coverage.[20] Additionally, the evaporation curves for both the monolayer and duolayer deviate from a linear relationship with time at the same point (~13 h from the start of the experiment), suggesting that both systems begin to lose C18E1 at the same time. This suggests that the observed improvement in water evaporation suppression by the duolayer system under wind is also due to changes in the molecular structure of the duolayer film itself.

In order for water to evaporate through the C18E1 film, the chains must be separated sufficiently to allow water molecules to pass between them.[23] Under an external force, we observed that the presence of the PVP in the duolayer system led to structural changes at the interface, with the C18E1 chains becoming denser, more ordered and the interaction between them becoming stronger. This would require a higher free energy to separate the chains, and will therefore lead to reduced evaporation under an external force (wind). Therefore, both mechanisms (1) and (2) contribute to the improved performance of the duolayer.

CONCLUSIONS

In this study, we used theoretical all-atom simulations to examine the effects of an applied force on the molecular structure and dynamics of monolayer and duolayer organic film systems for water evaporation protection. When the same constant force (with an added viscous drag to produce a constant velocity) is applied to the aliphatic chains of the monolayer and duolayer systems, a greater viscosity and slower average velocity are observed for the duolayer. This is due to the presence of PVP at the interface, and results in an increased film tilt, ordering, and hydrogen bond lifetime, which in turn yields a more dense C18E1 film. This greater film ordering and higher molecular density at the interface achieved in the duolayer under external force explains the experimentally observed increase in evaporation suppression efficacy of the duolayer system under wind.

AUTHOR INFORMATION

Corresponding Author

*Phone: (+613) 9925 2571. Fax: (+613) 9925 5290. E-mail: irene.yarovsky@rmit.edu.au.

Present Address

[§]IBM Research Australia, 5/204 Lygon St, Melbourne, Victoria 3001, Australia.

Notes

The authors declare no competing financial interest.

ACKNOWLEDGMENTS

This work has been funded by the Australian Research Council Discovery grant DP110101604. We acknowledge the generous allocation of high performance computational resources from the Australian National Computational Infrastructure (NCI), the Western Australian computational facility (iVEC), the Victorian Partnership for Advanced Computing (VPAC), and the Victorian Life Sciences Computational Initiative (VLSCI).

REFERENCES

(1) Arya, S. K.; Solanki, P. R.; Datta, M.; Malhotra, B. D. Recent advances in self-assembled monolayers based biomolecular electronic devices. *Biosens. Bioelectron.* **2009**, *24*, 2810−2817.

(2) Mani, G.; Chandrasekar, B.; Feldman, M. D.; Patel, D.; Agrawal, C. M. Interaction of endothelial cells with self-assembled monolayers for potential use in drug-eluting coronary stents. *J. Biomed. Mater. Res., Part B* **2009**, *90B*, 789−801.

(3) Aramaki, K.; Shimura, T. An ultrathin polymer coating of carboxylate self-assembled monolayer adsorbed on passivated iron to prevent iron corrosion in 0.1M Na2SO4. *Corros. Sci.* **2010**, *52*, 1−6.

(4) Kang, Z.; Liu, Q.; Liu, Y. Preparation and micro-tribological property of hydrophilic self-assembled monolayer on single crystal silicon surface. *Wear* **2013**, *303*, 297−301.

(5) Chinappi, M.; Casciola, C. M. Intrinsic slip on hydrophobic self-assembled monolayer coatings. *Phys. Fluids* **2010**, *22*, 042003−8.

(6) Pu, J.; Jiang, D.; Mo, Y.; Wang, L.; Xue, Q. Micro/nano-tribological behaviors of crown-type phosphate ionic liquid ultrathin films on self-assembled monolayer modified silicon. *Surf. Coat. Technol.* **2011**, *205*, 4855−4863.

(7) Gannon, G.; Greer, J. C.; Larsson, J. A.; Thompson, D. Molecular Dynamics Study of Naturally Occurring Defects in Self-Assembled Monolayer Formation. *ACS Nano* **2010**, *4*, 921−932.

(8) Hung, S.-W.; Hsiao, P.-Y.; Lu, M.-C.; Chieng, C.-C. Thermodynamic Investigations Using Molecular Dynamics Simulations with Potential of Mean Force Calculations for Cardiotoxin Protein Adsorption on Mixed Self-Assembled Monolayers. *J. Phys. Chem. B* **2012**, *116*, 12661−12668.

(9) Ahn, Y.; Saha, J. K.; Schatz, G. C.; Jang, J. Molecular Dynamics Study of the Formation of a Self-Assembled Monolayer on Gold. *J. Phys. Chem. C* **2011**, *115*, 10668−10674.

(10) Ramin, L.; Jabbarzadeh, A. Effect of Load on Structural and Frictional Properties of Alkanethiol Self-Assembled Monolayers on Gold: Some Odd−Even Effects. *Langmuir* **2012**, *28*, 4102−4112.

(11) Song, Y.; Luo, M.; Dai, L. L. Understanding Nanoparticle Diffusion and Exploring Interfacial Nanorheology using Molecular Dynamics Simulations. *Langmuir* **2009**, *26*, 5−9.

(12) Prime, E. L.; Leung, A. H. M.; Tran, D. N. H.; Harnam, G.; Solomon, D. H.; Qiao, G. G.; Dagley, I. New technology to reduce evaporation from large water storages. *Waterlines Report* 2012 (National Water Commission: Canberra, ACT).

(13) Rideal, E. K. On the influence of thin surface films on the evaporation of water. *J. Phys. Chem.* **1925**, *29*, 1581−1588.

(14) Barnes, G. T. The potential for monolayers to reduce the evaporation of water from large water storages. *Agric. Water Manage.* **2008**, *95*, 339−353.

(15) Prime, E. L.; Henry, D. J.; Yarovsky, I.; Qiao, G. G.; Solomon, D. H. Comb polymers: Are they the answer to monolayer stability? *Colloids Surf., A* **2011**, *384*, 482−489.
(16) Prime, E. L.; Tran, D. N. H.; Plazzer, M.; Sunartio, D.; Leung, A. H. M.; Yiapanis, G.; Baoukina, S.; Yarovsky, I.; Qiao, G. G.; Solomon, D. H. Rational design of monolayers for improved water evaporation mitigation. *Colloids Surf., A* **2012**, *415*, 47−58.
(17) Tran, D. N. H.; Prime, E. L.; Plazzer, M.; Leung, A. H. M.; Yiapanis, G.; Christofferson, A. J.; Yarovsky, I.; Qiao, G. G.; Solomon, D. H. Molecular interactions behind the synergistic effect in mixed monolayers of 1-octadecanol and ethylene glycol monooctadecyl ether. *J. Phys. Chem. B* **2013**, *117*, 3603−3612.
(18) Solomon, D. H.; Prime, E. L.; Sunartio, D.; Qiao, G.; Dagley, I.; Blencowe, A. *Method for Controlling Water Evaporation*; WO2010071931 A1; 2010.
(19) Prime, E. L.; Tran, D. N. H.; Leung, A. H. M.; Sunartio, D.; Qiao, G. G.; Solomon, D. H. Formation of Dynamic Duolayer Systems at the Air/Water Interface by using Non-ionic Hydrophilic Polymers. *Aust. J. Chem.* **2013**, *66*, 807−813.
(20) Leung, A. H. M.; Prime, E. L.; Tran, D. N. H.; Fu, Q.; Christofferson, A. J.; Yiapanis, G.; Yarovsky, I.; Qiao, G. G.; Solomon, D. H. Dynamic Performance of Duolayers at the Air/Water Interface. 1. Experimental Analysis. *J. Phys. Chem. B* **2014**, DOI: 10.1021/jp5060974.
(21) Yiapanis, G.; Christofferson, A. J.; Plazzer, M.; Weir, M.; Prime, E. L.; Qiao, G. G.; Solomon, D. H.; Yarovsky, I. Molecular mechanism of stabilization of thin films for improved water evaporation protection. *Langmuir* **2013**, *29*, 14451−14459.
(22) Theodorou, D. N.; Suter, U. W. Atomisitic Modeling of Mechanical Properties of Polymeric Glasses. *Macromolecules* **1986**, *19*, 139−154.
(23) Henry, D. J.; Dewan, V. I.; Prime, E. L.; Qiao, G. G.; Solomon, D. H.; Yarovsky, I. Monolayer Structure and Evaporation Resistance: A Molecular Dynamics Study of Octadecanol on Water. *J. Phys. Chem. B* **2010**, *114*, 3869−3878.
(24) Plimpton, S. Fast Parallel Algorithms for Short-Range Molecular Dynamics. *J. Comput. Phys.* **1995**, *117*, 1−19.
(25) PCFF is distributed along with Accelrys' software package Materials Studio. More information may be found on the Accelrys website: www.accelrys.com.
(26) Sun, H.; Mumby, S. J.; Maple, J. R.; Hagler, A. T. An ab Initio CFF93 All-Atom Force Field for Polycarbonates. *J. Am. Chem. Soc.* **1994**, *116*, 2978−2987.
(27) Chen, X. P.; Yuan, C. A.; Wong, C. K. Y.; Koh, S. W.; Zhang, G. Q. Validation of forcefields in predicting the physical and thermophysical properties of emeraldine base polyaniline. *Mol. Simul.* **2011**, *37*, 990−996.
(28) De Leener, C.; Hennebicq, E.; Sancho-Garcia, J.-C.; Beljonne, D. Modeling the Dynamics of Chromophores in Conjugated Polymers: The Case of Poly(2-methoxy-5-(2′-ethylhexyl)oxy 1,4-phenylene vinylene) (MEH-PPV). *J. Phys. Chem. B* **2009**, *113*, 1311−1322.
(29) Díaz, I.; Díez, E.; Camacho, J.; León, S.; Ovejero, G. Comparison between three predictive methods for the calculation of polymer solubility parameters. *Fluid Phase Equilib.* **2013**, *337*, 6−10.
(30) Chunsrivirot, S.; Trout, B. L. Free Energy of Binding of a Small Molecule to an Amorphous Polymer in a Solvent. *Langmuir* **2011**, *27*, 6910−6919.
(31) Deshmukh, S. A.; Li, Z.; Kamath, G.; Suthar, K. J.; Sankaranarayanan, S. K. R. S.; Mancini, D. C. Atomistic insights into solvation dynamics and conformational transformation in thermo-sensitive and non-thermo-sensitive oligomers. *Polymer* **2013**, *54*, 210−222.
(32) Pei, Y.; Ma, J.; Jiang, Y. Formation Mechanisms and Packing Structures of Alkoxyl and Alkyl Monolayers on Si(111): Theoretical Studies with Quantum Chemistry and Molecular Simulation Models. *Langmuir* **2003**, *19*, 7652−7661.
(33) Naik, V. V.; Vasudevan, S. Conformational Dynamics in Alkyl Chains of an Anchored Bilayer: A Molecular Dynamics Study. *J. Phys. Chem. B* **2009**, *113*, 8806−8813.
(34) Chen, Y.-J.; Xu, G.-Y.; Yuan, S.-L.; Sun, H.-Y. Molecular dynamics simulations of AOT at isooctane/water interface. *Colloids Surf., A* **2006**, *273*, 174−178.
(35) Hu, L.; Zhang, L.; Hu, M.; Wang, J.-S.; Li, B.; Keblinski, P. Phonon interference at self-assembled monolayer interfaces: Molecular dynamics simulations. *Phys. Rev. B* **2010**, *81*, 235427.
(36) Pang, J.; Wang, Y.; Xu, G.; Han, T.; Lv, X.; Zhang, J. Molecular Dynamics Simulations of SDS, DTAB, and C12E8Monolayers Adsorbed at the Air/Water Surface in the Presence of DSEP. *J. Phys. Chem. B* **2011**, *115*, 2518−2526.
(37) Hockney, R. W.; Eastwood, J. W. *Computer Simulation Using Particles*; Adam Hilger: New York, 1989.
(38) Nose, S. A Unified Formulation of the Constant Temperature Molecular-Dynamics Methods. *J. Chem. Phys.* **1984**, *81*, 511−519.
(39) Hoover, W. G. Canonical Dynamics - Equilibrium Phase-Space Distributions. *Phys. Rev. A* **1985**, *31*, 1695−1697.
(40) Rapaport, D. C. Hydrogen bonds in water. *Mol. Phys.* **1983**, *50*, 1151−1162.
(41) Phongikaroon, S.; Judd, K. P. Surfactant Effects on the Free Surface Thermal Structure and Subsurface Flow in a Wind-Wave Tunnel. *J. Fluids Eng.* **2006**, *128*, 913−920.
(42) Yoshizawa, H.; Chen, Y. L.; Israelachvili, J. Fundamental mechanisms of interfacial friction. 1. Relation between adhesion and friction. *J. Phys. Chem.* **1993**, *97*, 4128−4140.
(43) Lorenz, C. D.; Chandross, M.; Grest, G. S.; Stevens, M. J.; Webb, E. B. Tribological Properties of Alkylsilane Self-Assembled Monolayers. *Langmuir* **2005**, *21*, 11744−11748.
(44) Briscoe, W. H.; Klein, J. Friction and Adhesion Hysteresis between Surfactant Monolayers in Water. *J. Adhes.* **2007**, *83*, 705−722.
(45) Briscoe, W. H.; Titmuss, S.; Tiberg, F.; Thomas, R. K.; McGillivray, D. J.; Klein, J. Boundary lubrication under water. *Nature* **2006**, *444*, 191−194.
(46) Kaganer, V. M.; Peterson, I. R.; Kenn, R. M.; Shih, M. C.; Durbin, M.; Dutta, P. Tilted phases of fatty acid monolayers. *J. Chem. Phys.* **1995**, *102*, 9412−9422.
(47) Vollhardt, D.; Siegel, S.; Cadenhead, D. A. Characteristic Features of Hydroxystearic Acid Monolayers at the Air/Water Interface. *J. Phys. Chem. B* **2004**, *108*, 17448−17456.
(48) Shih, M. C.; Durbin, M. K.; Malik, A.; Zschack, P.; Dutta, P. Lattice structures and molecular tilts in Langmuir monolayers of saturated fatty acid−alcohol mixtures. *J. Chem. Phys.* **1994**, *101*, 9132−9136.
(49) Ghaskadvi, R. S.; Ketterson, J. B.; Dutta, P. Nonlinear Shear Response and Anomalous Pressure Dependence of Viscosity in a Langmuir Monolayer. *Langmuir* **1997**, *13*, 5137−5140.